

## METAL-COMPOSITE PIPES FOR DEEPWATER APPLICATIONS

### S.C.Oliveira Jr

COPPE/UFRJ – Centro de Tecnologia – Bloco I/2000-sala108  
e-mail – [carvalho@lts.coppe.ufrj.br](mailto:carvalho@lts.coppe.ufrj.br)

### I.P.Pasqualino

COPPE/UFRJ – Centro de Tecnologia – Bloco I/2000-sala108  
e-mail – [ilson@lts.coppe.ufrj.br](mailto:ilson@lts.coppe.ufrj.br)

### T.A.Netto

COPPE/UFRJ – Centro de Tecnologia – Bloco I/2000-sala108  
e-mail – [tanetto@lts.coppe.ufrj.br](mailto:tanetto@lts.coppe.ufrj.br)

**Abstract.** *This paper presents a new conception for submarine pipes, herein called metal-composite pipe, as an alternative for deepwater applications where thermal insulation and structural behavior requirements must be met. Three specimens laminated through the vacuum-bag process using aluminum for the inner pipe and fiber glass (woven roving) for the outer pipe were manufactured. The structural behavior under hydrostatic pressure is investigated with the aid of simplified models tested into a hyperbaric chamber filled with fresh water. The experimental results are compared with numerical models using the commercial FEM code ABAQUS, comprising non-linear analysis with three dimensional solid elements. In addition, the effect of adhesion or non-adhesion between the layers is considered. Uniaxial tension tests and the so-called two-rail shear tests are conducted to determine the material properties of the material. After calibrated, the numerical model is used to perform a parametric study comprising combinations of stacking sequence such as  $[0^\circ]$ ,  $[90^\circ]$ , symmetric  $[45^\circ/-45^\circ]$ s and cross-ply  $[0^\circ/90^\circ]$ s so as to assess the technical feasibility of this conception.*

**Keywords:** *Composite pipe; fiber reinforced, submarine pipe; collapse pressure.*

### 1.-Introduction

Flexible and rigid pipes (Novitsky and Gray, 2003) have been widely used for the development of ultra-deep water fields. Nevertheless, economical and operational parameters have been increasingly demanding the use of new materials like reinforced fibers or aluminum and titanium alloys, which can reduce significantly the weight of the structure. Nowadays, the development of new materials has become the great challenge of researchers and companies (Saliés, 2003). Different configurations like the sandwich pipe (Netto *et al.*, 2002 and Pasqualino *et al.*, 2002), the pipe-in-pipe (Bokaian, 2004) or hybrid riser systems (Hatton, 1997) have been proposed as a feasible alternative for flowlines (Gilchrist, 2001) and risers (Metivaud *et al.*, 1993).

The main objective of this study is to investigate the performance of a composite material in conjunction with a metal pipe under external pressure (Figure 1). The studied geometry comprises a metallic pipe with an extra outer layer of composite material. The advantage of this metal-composite structure is that the composite layer provides both thermal insulation and further structural strength when coupled with the inner pipe. Three small scale samples were laminated through the vacuum-bag process using aluminum for the inner pipe and reinforced fiber glass (woven roving) for the composite layer. After the manufacturing process, they were tested under hydrostatic pressure until the collapse.



Figure 1 - Metal-composite pipe section

A numerical model based on finite element method was developed within the framework of the commercial software ABAQUS in order to reproduce the experimental results. The effects of hydrostatic pressure (Sridaharan and Kasagi, 1996) or delamination (Tafreshi, 2004) in the composite layer were not investigated through the FE model. The aluminum layer was assumed to be  $J_2$ -type elastic-plastic, finitely deforming solid with isotropic hardening. The composite layer was modeled as an orthotropic-linear-elastic solid. Uniaxial tension tests and the so-called two-rail shear tests were conducted to determine the material properties. Contact between the two materials was modeled to simulate perfect and partial adhesion between layers. A mesh sensitivity analysis was done to determine the best refinement. After calibrated, the numerical model was used to perform a parametric study in order to assess the technical feasibility of this conception. The effect of stacking sequence and thickness of the composite layer were investigated in conjunction with the  $D/t$  (diameter to thickness relation) parameter of the metallic layer.

## 2 – Experiments

The pipe segments used to make the small-scale specimens were cut out from aluminum tubes of 5m length. The nomenclature used to identify these specimens is presented below:

ALXXYZ

where,

XX is the nominal diameter to thickness ratio of the tube;

Y is the number of the pipe string;

Z represents the different specimens cut out from the same string, i.e. A to E.

The total length of the specimens was equal to 975 mm. Their external surfaces were mapped in 13 transverse sections along the length and 20 points in the circumferential direction to determine average diameters and thicknesses. Table 1 shows the main measured geometric parameters, where  $D$  is the external diameter,  $t$  is the thickness and  $\Delta_o$  is the maximum value of initial ovalization.

$$\Delta_o = \frac{D_{\max} - D_{\min}}{D_{\max} + D_{\min}} \quad (1)$$

Table 1 – Main geometric parameters of the metallic tubes

Specimen	$D$ (mm)	$t$ (mm)	$D/t$	$\Delta_o$ (%)
AL381A	76.203	2.175	35.04	0.27
AL381B	76.187	2.185	34.87	0.30
AL381C	76.229	2.143	35.65	0.31
AL381D	76.190	2.153	35.43	0.28
AL381E	76.195	2.154	35.37	0.28

In the next step, three tubes (C, D and E) were laminated through the vacuum-bag process. A mechanical apparatus was used to fix the tubes by the edges, in order to assist the lamination process. Initially, the necessary portion of glass fabric to obtain the desired thickness is reserved. The epoxy resin is then applied on the tube external surface. Afterward, the fabric is placed around the pipe surface while further resin is applied with the aid of a roller to ensure thorough impregnation and wetting of the fibers. The composite of fiber-resin plies is first covered manually with a treated nylon called peel ply, which will confer the external texture of the specimen, and a layer of acrylon (bleeder). The aim of the acrylon is to absorb excess resin and allow volatiles vent. Later, the composite is covered with a partially perforated film which provides easy release and vacuum access to the laminate, then air bubbles plastic, which confer a layer capable to distribute the pressure around the specimen. Finally, the set is covered with a plastic-bag and sealed at the ends. A vacuum pump is used to keep the whole system at a pressure of approximately 1 atm while the resin is allowed to cure at room temperature. At the end of the manufacturing process, the plastics and peel ply layers are removed and the specimen is mapped once more (Figure 2).



Figure 2 – Laminated tube

A rubber-like sealing product was applied over the pipe surface, in order to prevent the water permeation in the laminate but nothing was used to enhance adhesion between layers (metal and composite). The specimen is sealed on their edges with the aid of cylindrical steel plugs provided with rubber o-rings. The set is positioned into a 10,000 psi hyperbaric chamber, which is completely filled with fresh water and pressurized using a positive displacement pump. The pressure is monitored by an electrical pressure transducer connected to the experimental setup. The pressure is increased until the collapse which is characterized by a strong noise followed by a sudden drop in pressure. Table 2 lists the collapse pressure ( $P_{co}$ ) of the five specimens tested, along with the main average geometric parameters of the aluminum-only (AL381A, AL381B) and laminated specimens (AL381C, AL381D, AL381E).

Table 2 – Summary of the experimental results

Specimen	$D$ (mm)	$t$ (mm)	$t_c$ (mm)	$P_{co}$ (MPa)
AL381A	76.203	2.175	-	3.32
AL381B	76.187	2.185	-	3.25
AL381C	76.229	2.143	3.784	6.39
AL381D	76.190	2.153	1.927	3.91
AL381E	76.195	2.154	4.982	15.83

A sample composite plate was manufactured likewise the laminate of the small-scale pipe specimens, so that test coupons based on ASTM specification D3039 (2002) could be extracted to evaluate tensile properties such as Young Modulus ( $E$ ) and Poisson ratio ( $\nu$ ). In addition, tests coupons were also manufactured using the fast impregnated resin, based on ASTM specification D638 (1994), so that its average tensile properties could be obtained. The resulting properties are displayed in Table 3. The average true stress-strain curve of aluminum (Figure 3) was also determined from uniaxial tensile test coupons.

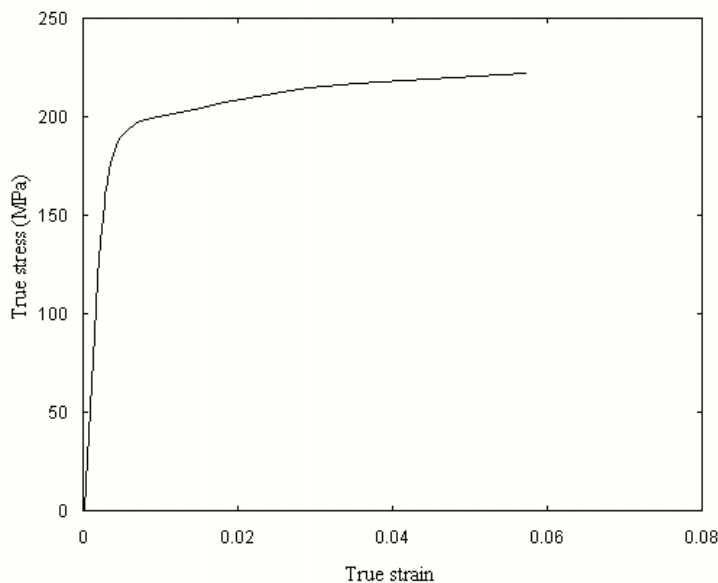


Figure 3 – True stress-strain curve of the aluminum

Table 3 – Average material properties of composite and resin

Material	$E$ (GPa)	$\nu$	$G_{12}$ (GPa)
Composite	20.42	0.1	2.52
Resin	2.544	0.12	-

Based on ASTM D4255 (2004), the average shear stress-strain curve of the composite materials is obtained through the rail shear test (Figure 4). It is carried out using a flat rectangular plate specimen, clamped between two rail fixtures, and subjected to uniaxial loading in a servo-hydraulic frame. This tension load generates in-plane shear stress along the specimen and the resulting strains are monitored by two opposite strain gages positioned at an angle of 45 degrees in relation to the longitudinal axis of the plate. Figure 5 shows the resulting configuration of the plate specimen. The gages registered a shear strain of approximately 8% before rupture (Figure 6). Table 3 lists the average in-plane shear modulus ( $G_{12}$ ) which is determined calculating the angular coefficient of the linear portion of the shear stress-strain curve.



Figure 4 – Two-rail fixture

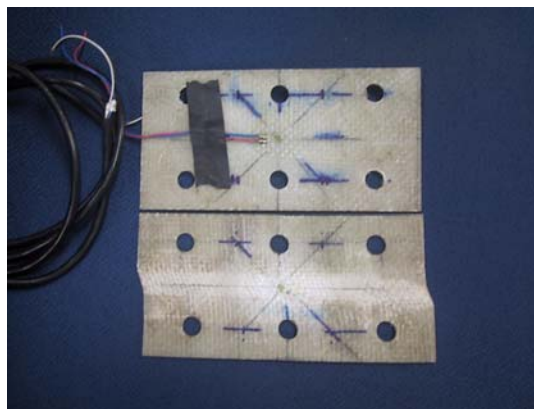


Figure 5 - Specimen test

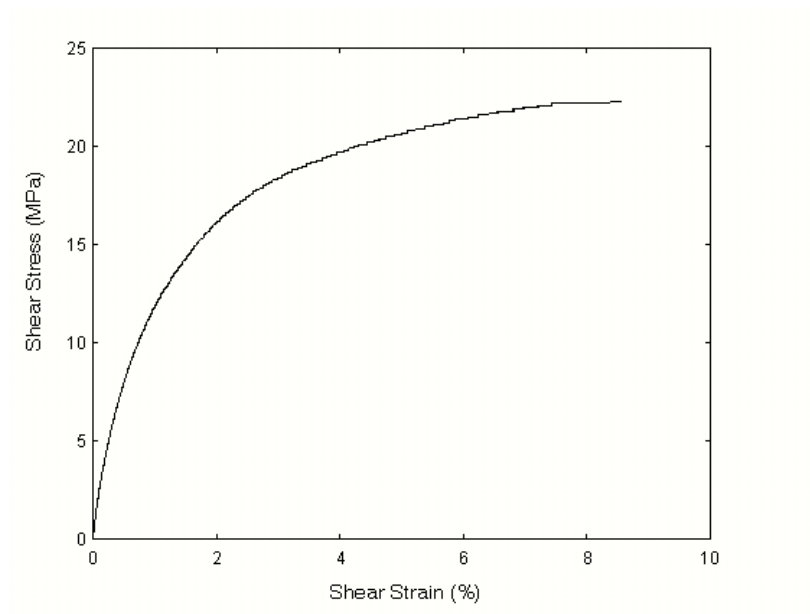


Figure 6. Shear stress-strain curve of the laminate

### 3 – Numerical Analysis

A numerical model based on the finite element method was developed within the framework of the commercial software ABAQUS, so as to simulate the behavior of sandwich pipes under external pressure. Twenty-seven-node, quadratic, three-dimensional solid elements (C3D27) with three degrees-of-freedom per node (displacements in 1, 2 and 3 directions) were used to model the inner (aluminum) and outer (laminate) layers. Symmetry conditions reduce the problem to one fourth of the original geometry. Inner and outer layers were discretized with 12 elements in the hoop direction, 2 elements through the thickness and 24 elements in the axial direction as shown in Figure 7. Furthermore, two layer interface conditions were simulated numerically, i.e., perfect adhesion and no adhesion. First, laminate and aluminum meshes shared the nodes along its interface (perfect adhesion). In a second approach, a surface based contact model was used to simulate lack of adhesion. This approach also allows defining friction between the contact surfaces. The aluminum layer was assumed to be J2-type elastic-plastic, finite deforming solid with isotropic hardening. The composite layer was modeled as an orthotropic-linear-elastic solid.

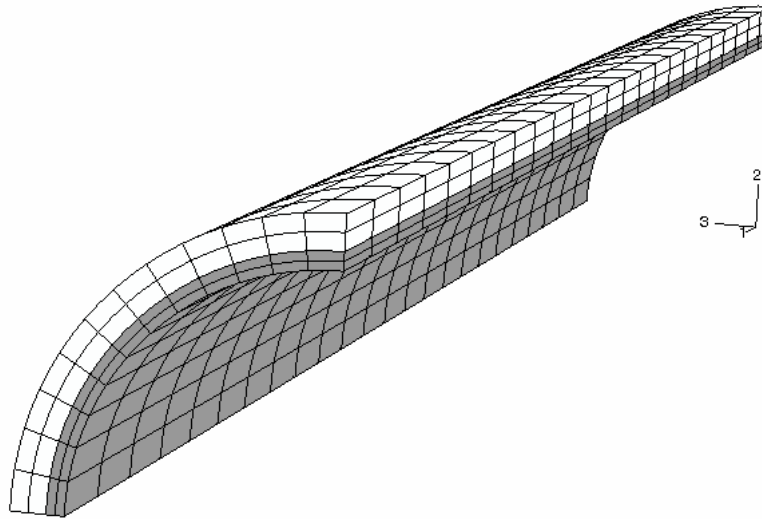


Figure 7 – Finite element mesh used in the analysis

Table 4 shows the material properties of the laminate. The properties through the thickness were assumed to be those of the resin, which is modeled as an isotropic material.

Table 4 – Average properties of the composite

Material	$E_{11}$ (GPa)	$E_{22}$ (GPa)	$E_{33}$ (GPa)	$\nu_{12}$	$\nu_{13}$	$\nu_{23}$	$G_{12}$ (GPa)	$G_{13}$ (GPa)	$G_{23}$ (GPa)
composite	2.54	20.42	20.42	0.12	0.12	0.1	1.14	1.14	2.52

The initial objective of the numerical method was to reproduce the experiments described above. The measured maximum initial ovalization ( $\Delta_o$ ) of the pipe (Table 1) was reproduced in the FEM via prescribing radial initial displacements ( $w_o$ ). The initial displacements are calculated with the aid of the following equation:

$$w_o(z, \theta) = -R \cdot \Delta_o \cdot e^{-\beta \left(\frac{z}{D}\right)^2} \cdot \cos(2\theta) \quad (3)$$

where,  $D$  is the outside diameter of the composite pipe,  $\theta$  is the polar coordinate of a given node ( $0 \leq \theta \leq 90^\circ$ ),  $R$  is the internal radius of the composite pipe,  $z$  is the coordinate of the node in direction 3 and  $\beta$  is an exponential parameter (interval between 0.1 and 1).

Table 5 shows the results of the analyses considering perfect adhesion and no adhesion between the aluminum and laminate layers. The numerical results with perfect adhesion overestimated the collapse pressure ( $P_{co}$ ) while the no adhesion model approximated the experimental results. The collapse pressure of AL381D and AL381E no adhesion model is 6.5% and 11.84% smaller than that of the experiment, respectively. On the other hand, the collapse pressure of AL381C model is 4.85% higher than the experimental value.

Further analysis considering different friction coefficients between the layers of the model AL381E were carried out. The increasing of the friction coefficient approximated the experimental results, as can be observed in Table 6.

Table 5 – Comparison between experimental and numerical results

Model	$P_{co}$ (MPa) – perfect adhesion	$P_{co}$ (MPa) – no adhesion	$P_{co}$ (MPa) –experiment
AL381D	8.47	3.67	3.91
AL381C	13.86	6.7	6.39
AL381E	24.80	11.84	15.83

Table 6 – AL381E model considering friction

Friction	$P_{co}$ (MPa) - friction	$P_{co}$ (MPa) - experiment
0.1	13.8	15.83
0.15	15.2	15.83
0.20	16.5	15.83

#### 4 – Parametric study

The main parameters investigated in this study were the influence of laminate lay-ups, which include four different types, i.e.,  $[0^\circ]$  in relation to the model circumferential direction,  $[90^\circ]$ , symmetric angle-ply laminate  $[45^\circ/-45^\circ]$  and cross-ply laminate  $[0^\circ/90^\circ]$ . It was adopted the X60 grade steel for the metallic inner pipe. E-glass fiber and the resin properties used in the experiments were adopted to define the FEM. The composite material was combined based on micromechanical theory described in Daniel *et al.* (1994). The external diameter of the inner pipe ( $D$ ) and thickness of the both layers  $t$  (steel) and  $t_c$  (composite) were varied and ovalization ( $\Delta_o$ ) of 0.2% was fixed. The geometric parameters considered in this study are given in Table 7.

Table 7 – Geometric parameters of metal-composite pipes analyzed

$D$ (mm)	$t$ (mm)	$t_c/t$	$\Delta_o$ (%)
168.3	7.11	1	0.5
219.1	6.35	1	0.5
273	6.35	1	0.5

Figure 9 illustrates the collapse pressure of different configurations for a composite pipe with adhesion between the layers. Considering the same  $D/t$  ratio, the configuration  $[0^\circ]$  showed to be more efficient against collapse, because the compressive hoop stresses dominate the failure under external pressure. Otherwise, the weakest configuration  $[90^\circ]$  could be more favorable in situations where the axial loading is predominant. In addition, symmetric configurations  $[45^\circ/-45^\circ]$  would prevail over shear loadings. Five different failure criteria were checked to the laminate layer, such as Azziz-Tsai-Hill, Tsai-Hill, Maximum Stress, Maximum Strain and Tsai-Wu (ABAQUS Manual, 2004). These failure criteria detected points of failure at the laminate just after the collapse pressure.

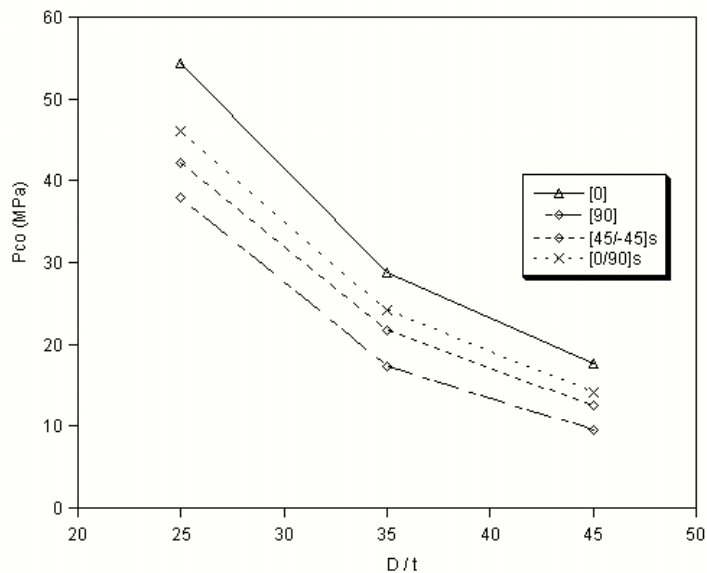


Figure 9 – Diagram of collapse pressure versus diameter to thickness ratio of the steel pipe



Further analyses were accomplished with the configuration  $[0^\circ]$ , considering the ratios  $t_c$  (laminate thickness) to  $t$  (steel thickness) equal to 0.5, 1, 1.5, 2, 2.5 and 3, respectively. Three different  $D$  (diameter) to  $t$  (thickness) ratios equal to 25, 35 and 45 were used. Figure 10 shows that the collapse pressure increases almost exponentially with increasing of thicknesses ratio ( $t_c/t$ ) for the same  $D/t$  ratio.

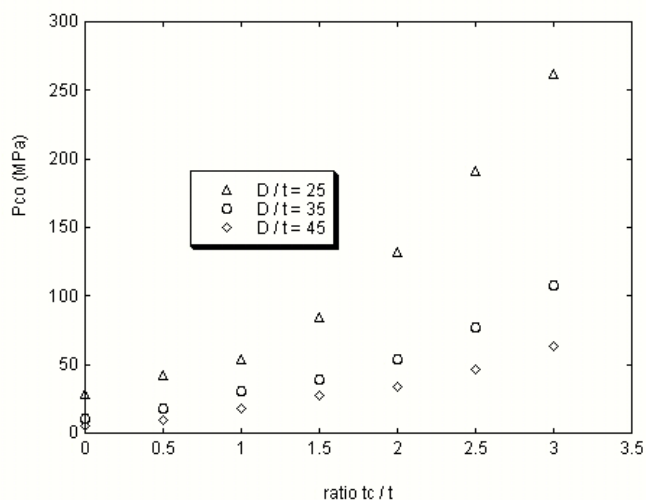


Figure 10 – Diagram of collapse pressure versus thickness of the laminate versus thickness of the steel layer for the configuration  $[0^\circ]$ .

## 5 – Conclusions

The collapse pressure of a metal-composite pipe conception was evaluated through a numerical and experimental study. Two different bonding conditions between metal and laminate layers were considered in the numerical analyses, perfect adhesion and non-adhesion. The numerical results considering non adhesion showed good correlation with the experiments, while the model with perfect adhesion overestimated the experimental results. In addition, a better correlation between numerical and experimental results is obtained when friction between layers is considered.

The effect of stacking sequence on the strength was investigated. Unidirectional fiber glass and X60 grade steel were adopted. Specimens with a  $[0^\circ]$ ,  $[90^\circ]$ , symmetric angle-ply laminate  $[45^\circ/-45^\circ]$  and cross-ply laminate  $[0^\circ/90^\circ]$  were subjected to hydrostatic external pressure. As expected, the results showed that maximum strength is achieved when aligning the fibers in the hoop direction only  $[0^\circ]$ . An average increase of 34.23% is observed when comparing the collapse pressures of specimens with  $[0^\circ]$  and  $[90^\circ]$  for  $D/t$  equal to 25.

It is clear that the composite layer significantly improves the collapse pressure of the pipe (Figure 10). For example, considering a pipe with  $D/t$  equal to 35, an increase of five times more than steel only was achieved when considering the composite thickness two times the pipe thickness ( $t_c/t = 2$ ).

For  $t_c/t = 3$ , the increase was 7.5 times. Even better results are obtained for pipes with lower  $D/t$ 's. For  $D/t=25$  the calculated increase for  $t_c/t = 3$  is 9.09 times.

## 6 – Acknowledgements

The authors would like to acknowledge the financial support from Brazilian National Petroleum Agency (ANP) and Submarine Technology Laboratory (LTS) - COPPE at different stages of this research work. The work of T.A.Netto was also supported by CNPQ. The technical support provided by the staff of the Submarine Technology Laboratory – COPPE is acknowledged with thanks.

## 7 –References

- Abaqus Manual, 2004, “ABAQUS / Standard user's manual”, Vol. II, Version 6.4, pp. 10.2.3-1- 10.2.3-4.
- ASTM.D3039, 2002, “Standard Test Method for Tensile Properties of Polymer Matrix Composite Materials”, Annual Book of ASTM Standards, Vol.15.03, pp. 114-123.
- ASTM. D4255, 2004, “Standard Guide for testing in-plane shear properties of composite laminates”, Annual Book of ASTM Standards, Vol.15.03, pp. 199-208.
- ASTM. , D638, 1994, “Standard Test Method for Tensile Properties of Plastic”, Annual Book of ASTM Standards, Vol.08.01, pp. 52-64.
- Bokaian, A., 2004, “Thermal expansion of pipe-in-pipe systems”, Marine Structures, Vol.17, pp. 475-500.

- Daniel, I.M. and Ishai, O., 1994, "Engineering Mechanics of Composite Materials", Ed. Oxford University Press, New York, USA, 395p.,
- Gilchrist, R., 2001, "Repairs of the Macaroni 10 x 6 in. Pipe-in-pipe flowline", Proceedings of the 20<sup>th</sup> Offshore Technology Conference ,OTC-13015, Houston, USA, pp. 1-10.
- Hatton, S.A., 1997, "Low Cost Deepwater Hybrid Riser System", Proceedings of the 24<sup>th</sup> Offshore Technology Conference , OTC-8523, Houston, USA, pp. 1-12
- Metivaud, G., 1993, "Composite Risers for deepwater applications", Oil & Gas Science and Technology, Vol.48, No.2, pp. 105-114.
- Netto, T.A., Santos, J.M.C. and Estefen, S.F., 2002, "Sandwich pipes for ultra-deep waters", Proceedings of the 4<sup>th</sup> International Pipeline Conference, IPC-27426, Calgary, Alberta, Canada, pp. 1-9
- Novitsky, A. and Gray, F., 2003, "Flexible and rigid pipe solutions in the development of ultra-deepwater fields", Proceedings of the 22<sup>nd</sup> International Conference on Offshore Mechanics and Arctic Engineering, OMAE-37401, Cancun, Mexico, pp. 1-15.
- Pasqualino, I.P., Pinheiro, B.C. and Estefen, S.F., 2002 "Comparative Structural Analyses Between Sandwich and steel Pipelines for Ultra-Deep Water", 21<sup>st</sup> International Conference on Offshore Mechanics and Arctic Engineering, June 23-28, Oslo, Norway.
- Saliés, J.B., 2003, " Procap-3000: New challenges for 3000m water depth", Proceedings of the 22<sup>nd</sup> International Conference on Offshore Mechanics and Arctic Engineering , OMAE-37399, Cancun, Mexico, pp. 1-8.
- Sridharan, S. and Kasagi, A., 1997, "On the buckling and collapse of moderately thick composite cylinders under hydrostatic pressure", Composites part B, Vol. 28, pp-583-596.
- Tafreshi, A., 2004, "Delamination buckling and postbuckling in composite cylindrical shells under external pressure", Thin-walled structures, Vol.42, pp. 1379-1404

#### **8 – Responsibility notice**

The author(s) is (are) the only responsible for the printed material included in this paper.